ACS OMEGA

http://pubs.acs.org/journal/acsodf

Article

Enhancing Gas Solubility in Water via Femtosecond Laser-Induced Plasma

Vadim Ialyshev, Ganjaboy Boltaev, Mazhar Iqbal, Mustafa Khamis, and Ali S. Alnaser*

Cite This: *ACS Omega* 2022, 7, 28182−28189

Read Online

ACCESS | Metrics & More | Article Recommendations

ABSTRACT: The generation of laser-induced plasma at the gas−liquid interface provides many fundamental and interesting scientific phenomena such as ionization, sharp explosion, shock wave radiation, bubble creation, and water splitting. However, despite the extensive research in this area, there is no reference on the effect of the surrounding environment on the chemical processes that occur during the laser-induced plasma−water interaction. In this work, we investigate the effect of the surrounding gas environment on femtosecond laser-induced plasma when generated at the pure water−gas interface. Ultrashort laser pulses were applied to water in the presence of air and N_2 and Ar gas environments. Formation of a significant number of nitrate-based species in water was observed after exposure to femtosecond laser-induced plasma in air and N_2 environments. The detected NO_3 ions formed in the laser-treated water led to the appearance of an absorption peak in the UV range, a significant decrease in the water pH value, and a significant increase in water's electrical conductivity. All induced properties of water were stable for 3 months of monitoring after laser treatment. Our work shows that the generation of laser-induced plasma in water propagating into a gaseous medium facilitates the interaction between the two media, as a result of which the compositions of substances present in the gaseous medium can be dissolved in water without increasing the gas pressure. The presented approach may find applications in areas such as water purification, material synthesis, and environmental stewardship.

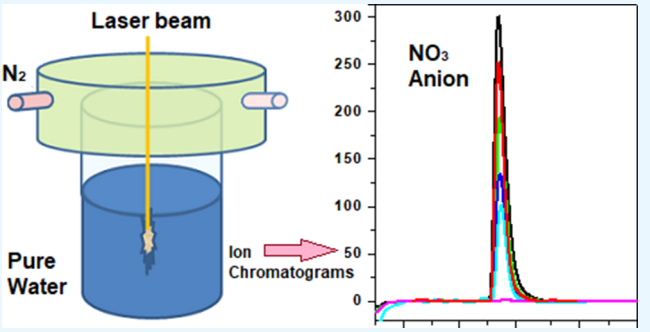

1. INTRODUCTION

Ultrafast lasers are used in many applications to modify the chemical, structural, and optical properties of materials.[1−4] The ultrafast nature and nonlinear interaction of a high-intensity laser with matter lead to a decrease in the zone of thermal influence with minimal collateral damage compared to the results achieved using continuous-wave or long-pulse lasers.[5] These properties allow us to precisely modify materials and to investigate ultrafast mechanisms during phase transitions or biochemical and chemical reactions.[1,6−9]

Laser irradiation of aqueous media plays an important role in many chemical[10,11] and atmospheric phenomena.[12] Photolysis of water is of paramount importance as it is one of the possible sources of fuel that can be obtained by the dissociation of water into hydrogen and oxygen.[13] It has been shown that plasma generated by ultrashort laser pulses, especially femtosecond pulses, can be used for the production of hydrogen.[14] Although the production of hydrogen by this method is yet uneconomical, femtosecond lasers have recently received considerable interest for their potential use in biological and medical applications with many exciting and promising results.[15,16] Laser-generated plasma in liquids opens exciting applications including reagent-free characterization of biological objects[17] and decontamination of polluted water.[18] These applications contributed significantly toward the development of research on the complex interactions between laser-induced plasma and liquid water. However, most of these studies were mainly interpreted on the basis of physical phenomena, and only few reports were devoted to the chemical processes that occur during the generation of femtosecond laser-induced plasma in pure water. Hence, in most of these studies, the generated products of such interactions were ignored despite their importance in biology and medicine.

Several comprehensive reviews have recently appeared in the literature on the interaction of nonequilibrium plasma with liquids.[19,20] A number of complex phenomena related to the plasma−water interaction have been developed in these reviews. It has been accepted that the production of reactive oxygen and closely related reactive nitrogen radicals plays a

Received: April 19, 2022
Accepted: July 22, 2022
Published: August 3, 2022

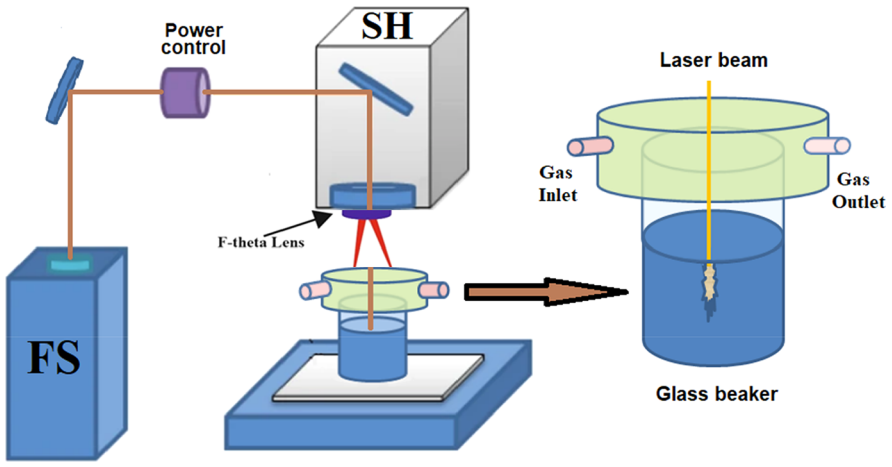

Figure 1. Experimental setup: movement of the beam from the femtosecond laser source (FS) was controlled by a scanning head (SH) and focused in water inside a glass beaker. The gas was fed into the beaker through an inlet port.

dominant role in plasma–water interaction processes. However, those previous studies were focused on the properties of plasma generated by four often used discharges: a pulsed direct discharge in a liquid, a DC air glow discharge with a water electrode, a pulsed plasma jet (nontouching), and a filamentary dielectric barrier discharge, and there was no reference related to laser-induced plasma interactions.[19]

Strong laser irradiation of water can cause intriguing phenomena such as plasma generation, shock wave radiation, splitting, and sharp explosions.[14,21,22] In addition, ionization of water leads to the generation of O^+, H^+, OH^+, and H_2O^+ radicals.[22] The thermalized radical and ionic species react with water molecules and other species in the solution, forming a variety of species such as H_2, H_2O_2, O_2, and so forth.[14,22,23] However, despite the extensive research in this area, there is no reference on the effect of the surrounding environment on the chemical processes that occur during the laser-induced plasma–water interaction.

The actual effect of a plasma–air–water interaction is ultimately determined by the generated chemical species and their diffusions, which are in turn determined by the laser (electric field and photons), ions, and electron fluxes and energies. It is clear that a more fundamental understanding of the processes occurring both in water and at its boundary with the atmosphere, when exposed to a laser, will eventually lead to a wider use of femtosecond lasers in water purification as well as other fields.

Recently, significant efforts have been made to develop new methods of water purification from hazardous organic waste. Methods such as the irradiation of waste or the use of supercritical oxidation of water have been proposed.[24] OH is a strong oxidant, so the generation of OH in the treatment process can rapidly oxidize various organic compounds in wastewater. Generating laser-induced plasma in the air–water interface area can involve both physical (ionization, shock waves, cavitation effects, and photolysis) and chemical (formation of reactive species and oxidation of organic contaminants) effects that play significant roles in the decomposition of organic contaminants. Thus, the effect of the laser-induced plasma, on the one hand, can create a large number of radicals directly in water and, on the other hand, can introduce reactive species from the environment, the amounts of which can be controlled by adjusting the laser treatment parameters.

In this work, we study the influence of the environment on the processes occurring in water during the generation of laser-induced plasma near the gas–water interface. Laser-induced plasma is generated in pure water in the presence of various gaseous media, such as air, N_2, and argon. To characterize and quantify the changes occurring in water after the interaction with plasma, UV–vis spectroscopy and ion chromatography (IC) were employed. Significant changes in the optical absorption, pH, and electrical conductivity were detected in water after treatment with laser-induced plasma in the presence of air or nitrogen gas. IC analysis showed the presence of a large number of nitrate ions, which were formed in water due to the interaction of gaseous nitrogen molecules with plasma at the water surface. We found that the formation process of nitrate ions is significantly affected by the position of the laser beam focus and the laser exposure time. We demonstrate that the generation of laser-induced plasma in water near its surface contributes to a significant dissolution of substances present in the gaseous medium just above the water surface while not requiring (according to Henry's law) an increase in gas pressure. Improving the understanding of the physical and chemical processes in the field of the plasma–liquid–gas interaction will find applications in a wide range of fields, including the science of aerosols, atmospheric and colloidal chemistry, phase equilibrium and gas/liquid solubility, biology, water purification, and environmental protection.

2. EXPERIMENTAL SECTION

Femtosecond laser pulses were generated using a Yb-doped fiber laser system (UFFL-300-2000-1030-300, Active Fiber Systems GmbH) with a central wavelength of 1030 nm and a repetition rate of 50 kHz. An average power of 10 W and a pulse duration of 40 fs were used for the irradiation of liquid water.[25] The laser beam was directed to a computer-driven galvanometric scanning head (FARO tech., Xtreme-20) that controlled the movement of the beam at a speed of 300 mm/s and a scanning interval of 50 μm. Laser radiation was focused using a 160 mm F-Theta lens, which provided a spot diameter of approximately 100 μm and a laser-scanned area of 20 × 20 mm^2. The scanning beam was directed through a quartz window inside a glass beaker (40 mm in diameter) that contained 30 mL of deionized water. Water purified in a Millipore Elix5/Milli-Q system (a specific resistance > 18.2

https://doi.org/10.1021/acsomega.2c02384
ACS Omega 2022, 7, 28182–28189

MΩ·cm and a pH of 6.4) was used in all experiments. The position of the glass beaker was fixed in a special holder during the irradiation experiments. The focus position of the laser beam was varied by up−down movements of the holder. Air and N_2 and Ar gases with 99.95% purity flowed continuously through a cap with a flow rate of 2 L/min. Figure 1 shows a sketch of the experimental setup.

To study the influence of the environment, a cap was placed on the glass beaker through which the corresponding gas flowed. A double-beam UV−vis−NIR spectrophotometer (Unicam Helios Alpha) was used in the optical absorbance measurement mode. The U-4100 model was used for the measurement of a broad range of wavelengths that extended from 200 to 2500 nm; the U-3900 model was used for shorter wavelength measurements up to 190 nm over a narrower range of 800 nm. The spectrophotometer was operated with a fixed spectral resolution of 2 nm. The measurements were performed in quartz cuvettes. Inorganic ions were determined using a Shimadzu Prominence ion chromatograph system (Japan) equipped with a conductivity detector. Sodium carbonate (Na_2CO_3) and sodium hydrogen carbonate ($NaHCO_3$) from Sigma-Aldrich were used for the preparation of eluents (1.8 mmol/l Na_2CO_3 + 1.7 mmol/l $NaHCO_3$). Standard solutions of anions (F^-, Cl^-, NO_2^-, NO_3^-, PO_4^{3-}, and SO_4^-) and cations (Na^+, K^+, Mg^{2+}, and Ca^{2+}) were prepared with Sigma-Aldrich reference solutions. Calibration solutions were made by diluting appropriate standard solutions right before their application. All solutions were kept in glass or high-density polyethylene containers at room temperature. Electrical conductivity and pH were measured using an HI 2300 EC/TDS/NaCl meter (HANNA Instruments, USA) and the Hach sensION+ (Thomas Scientific, USA), respectively.

3. RESULTS AND DISCUSSION

3.1. Effect of the Focus Position on UV Absorbance. The first step in studying the interaction of water with the femtosecond laser beam was to determine how the properties of water changed depending on the position of the laser-beam focus. The irradiation was carried out under an ambient atmosphere with a fixed time of 20 min and a laser intensity of 6×10^{13} W/cm^2 to produce continuous plasma. The position of the laser focus was determined by the plasma glow at the lowest laser power. The optical absorption of the samples was measured after laser exposure. Figure 2a shows the typical absorption spectra of water where the laser-beam focus position was varied from 0 mm (water surface) to a depth of 20 mm under the water surface. A broad absorbance peak appeared in the UV region of the spectrum, and no signal was detected at the longer wavelength. As can be seen from Figure 2b, the intensity of the absorbance peak increased as the focus moved deeper from the surface, reaching a maximum absorbance value at a position of 5 mm. With further immersion of the focus, the intensity of the absorption signal decreased significantly. These results clearly show that the position of plasma in water is one of the important parameters in the formation of active radicals in water.

3.2. Effect of the Environment on UV Absorbance. In order to investigate the effect of the environment on the femtosecond laser-induced plasma−water interaction, the glass beaker was tightly closed with a cap through which air and N_2 and Ar gases flowed. All samples were irradiated using the same laser parameters and exposure time and a focus position at 5 mm. Figure 3 displays the spectra obtained under each condition.

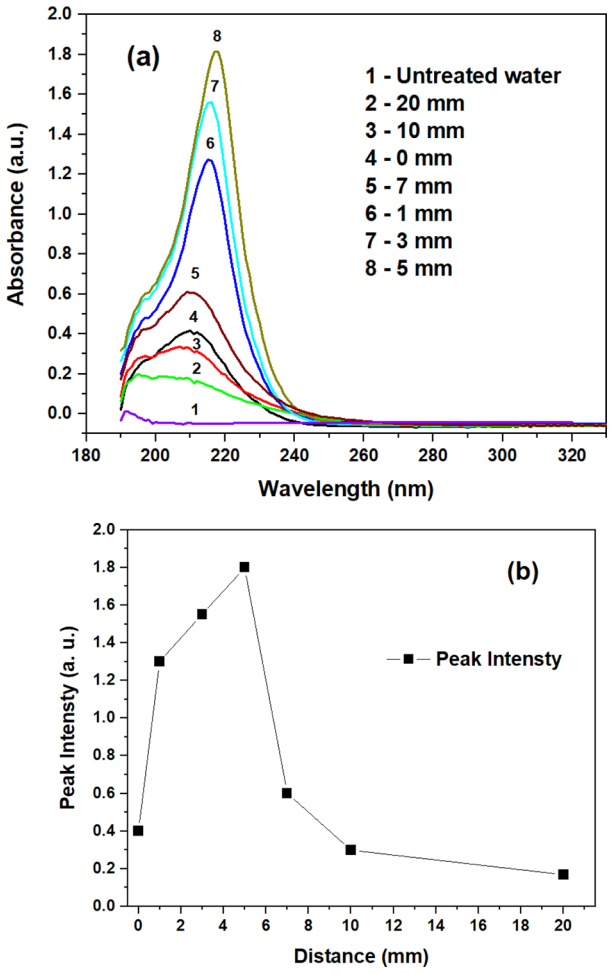

Figure 2. (a) Typical UV spectra of laser-treated water in an air environment at different laser-beam focus positions. (b) Absorbance peak intensity plotted as a function of focus position.

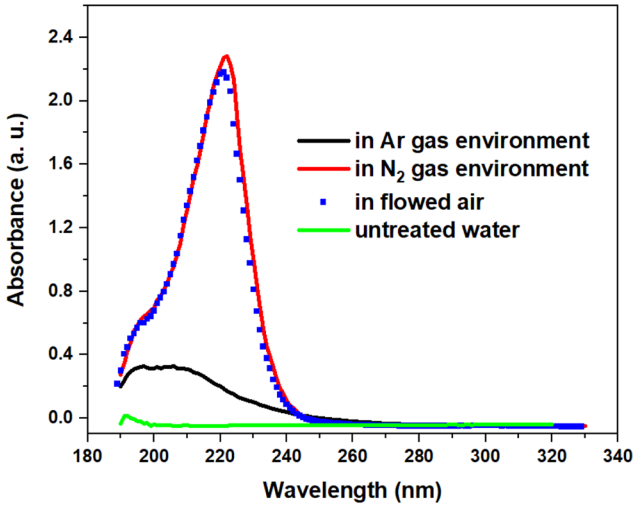

Figure 3. UV spectra of water irradiated by a femtosecond laser under different environment conditions: untreated water (green), air flow (blue dots), argon flow (black line), and nitrogen flow (red line). The exposure time is 20 min, the laser power is 10 W, and the gas flow rate is 2 L/min.

https://doi.org/10.1021/acsomega.2c02384
ACS Omega 2022, 7, 28182−28189

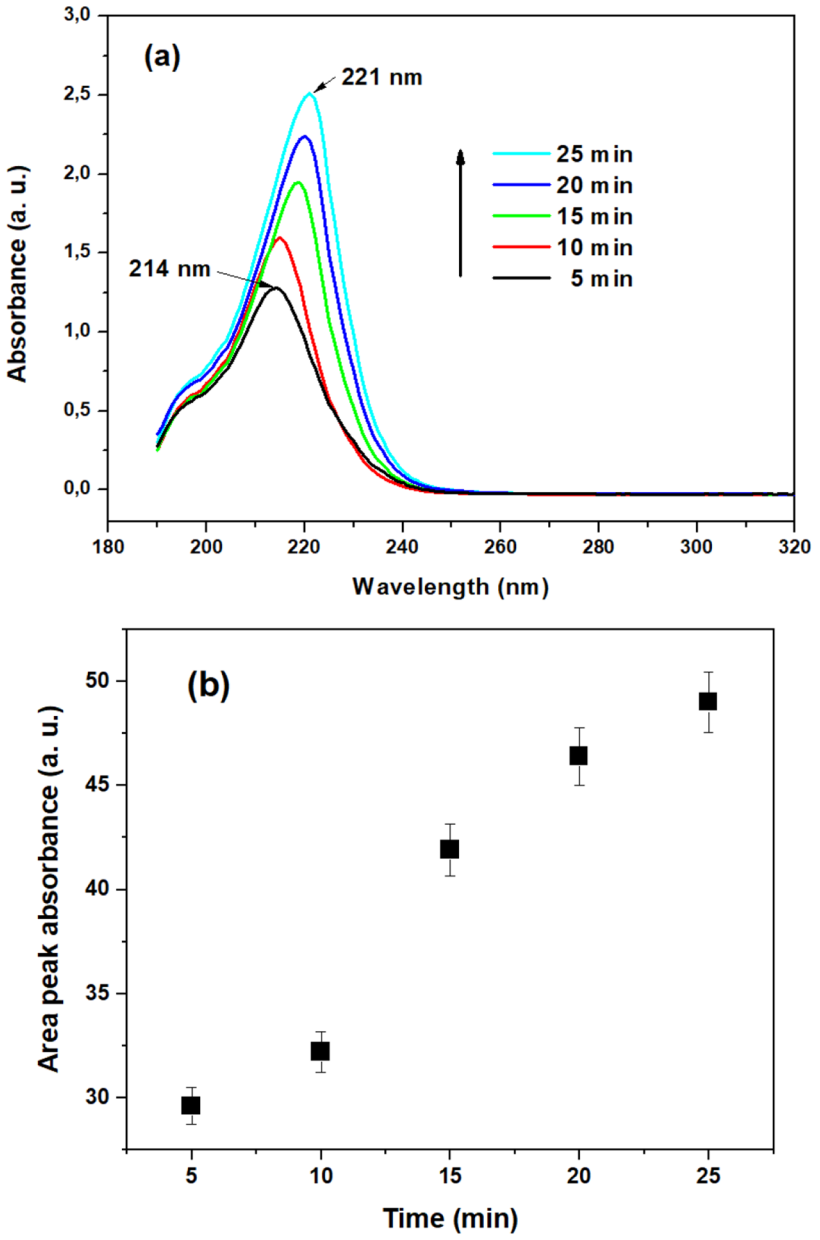

Figure 4. (a) UV absorption spectra of water irradiated with the femtosecond laser (a power of 10 W; a gas flow rate of 2 L/min, and a focus position of 5 mm) for different exposure times. (b) Plot of the absorbance peak areas vs laser exposure time.

Inspection of Figure 3 reveals that a strong absorbance peak is observed when irradiation was carried out in flowing air and N_2 gas. However, a much weaker peak is obtained in the case of Ar gas. Furthermore, irradiation of the water samples under an air or nitrogen flow gave the same absorbance value at $\lambda_{max} \sim 220$ nm. This clearly points out that the most likely candidate responsible for the appearance of the strong peak is nitrogen gas, which could be dissolved in water during the interaction with the femtosecond laser. It is worth mentioning that the obtained absorbance in Figure 3 is significantly higher than that obtained in Figure 2 under static air irradiation. This increase could be explained by the removal of water vapor that occurs during the laser treatment, which tends to reduce the laser energy and hence its effectiveness in water photolysis.

3.3. Effect of the Exposure Time on UV Absorbance. Figure 4a shows the spectra of water irradiated for different exposure times at a fixed focus position of 5 mm under flowing air. Inspection of this figure reveals that the intensity of the absorption spectra increased with increasing laser exposure time with a simultaneous increase in λ_{max} from 214 to 221 nm. Upon analyzing the data for the exposure time dependence of the peak areas, it was found that the absorbance increased nonlinearly. It can be seen from Figure 4b that the intensity of the absorbance peak increased nonlinearly with increasing laser exposure time. It should be mentioned that the intensity of the absorbance peaks did not change even after 3 months.

3.4. Content Analysis. To identify the species formed in water after laser exposure, the samples were analyzed by the IC method. Figure 5a shows chromatogram examples for the water samples irradiated for different exposure times at a focus position of 5 mm and under flowing air and Ar gas. These measurements revealed that only one signal, which corresponds to the NO_3 anion, was observed from the water treated under flowing air. The intensity of the peak increased with

https://doi.org/10.1021/acsomega.2c02384
ACS Omega 2022, 7, 28182−28189

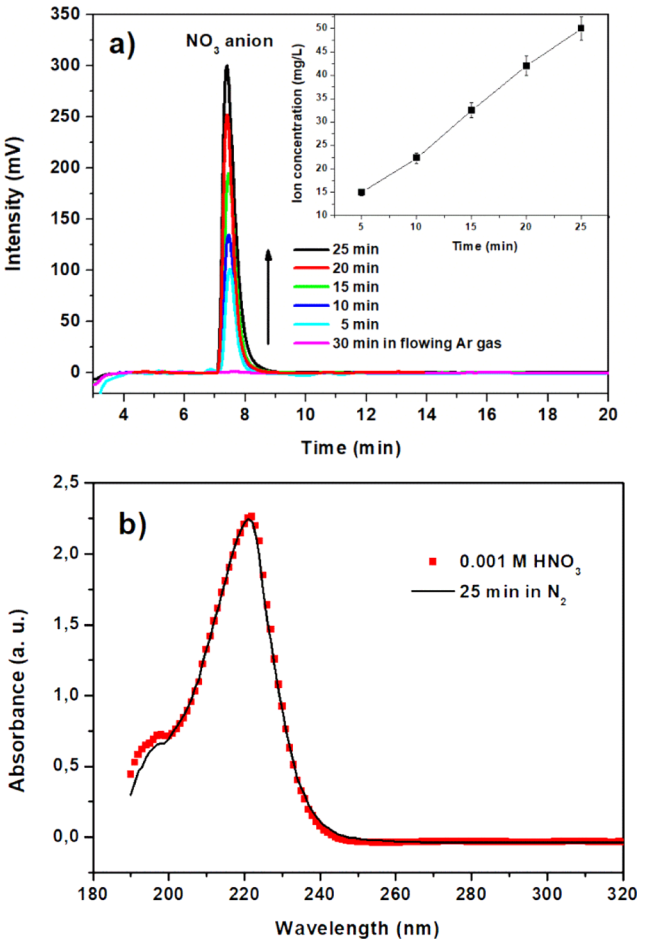

Figure 5. (a) Ion chromatograms of water irradiated for different exposure times under flowing air and Ar gas. The inset shows the ion concentration curve. (b) Comparative UV absorption spectra of water irradiated in N_2 for 25 min and nitric acid with a molarity of 0.001 M.

increasing laser exposure time. The calculated concentration of the nitrate species in the laser-treated water irradiated for 25 min was about 50 mg/L. At the same time, no signals were detected from the water treated under flowing Ar gas.

The results of pH and electrical conductivity measurements of the treated samples showed an increase in water acidity and electrical conductivity as laser exposure increases. As can be seen from Table 1, after 5 min of irradiation, water acquires acidic properties. For comparison, the absorbance spectrum and pH/conductivity data of nitric acid with a molarity of 0.001 M are shown in Figure 5b and Table 1, respectively.

3.5. Discussion. The laser parameters used in this work (a laser power of 10 W and a pulse duration of 40 fs) together with a diameter of the focused laser spot of 100 μm yielded to an intensity on the order of 10^{13} W/cm^2. Such a high-intensity ultrashort (fs) laser pulse allows for the generation of plasma through ionization of water by multiphoton absorption and by cascade ionization. The plasma creates a wide range of chemical particles and physical effects, which include radical

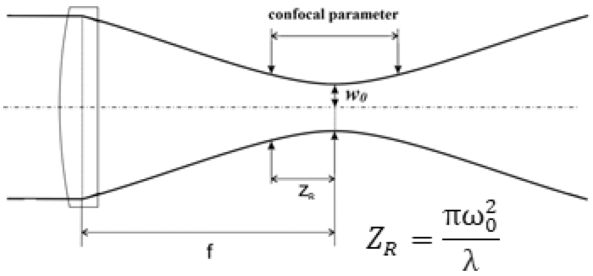

Figure 6. Rayleigh length criterion. Z_R is the Raleigh length, w_0 is the waist radius, and f is the focal length.

and reactive particles, ions, electrons, UV radiation, electric fields, heat, and shock waves. The basic chemical reactions that occur during the generation of femtosecond laser-induced plasma in pure liquid water are given in eqs 1−5.[22,26,27]

$$H_2O + h\nu \rightarrow H_2O^* \rightarrow H^\bullet + OH^\bullet \quad (1)$$

$$H^\bullet + H_2O \rightarrow H_3O^+ + e^- \text{ (hydrated)} \quad (2)$$

$$H^\bullet + OH^\bullet \rightarrow H_2O \quad (3)$$

$$2H^\bullet \rightarrow H_2 \quad (4)$$

$$2OH^\bullet \rightarrow H_2O_2 \quad (5)$$

On the other hand, the formation of long-lived chemical products (O_3, H_2O_2, NO_3^-, and NO_2^-) in water was shown to be produced by a gaseous discharge plasma at the gas−liquid interface.[20,24,28,29] Furthermore, these studies revealed that nitrogen products could be formed in water through the dissolution of nitrogen oxides formed in air plasma by gas-phase reactions of the dissociated N_2 and O_2 as given in eqs 6−9.[19,24,28,29]

$$N_2 + O_2 + e^* \rightarrow 2NO + e \quad (6)$$

$$2NO + O_2 \rightarrow 2NO_2 \quad (7)$$

$$NO + OH \rightarrow HNO_2\ (aq) \quad (8)$$

$$NO_2 + OH \rightarrow HNO_3\ (aq) \quad (9)$$

The generated reactive species in the gaseous phase move to the liquid phase by convection and diffusion. The parameters that control the solubility of the gaseous species at the water interface are affected by the ratio of species concentrations in the gas and liquid at the interface and by the Henry's law coefficient (k_H).[19] Species that have low values of k_H display low solubility and hence are difficult to be transferred from the gas to the liquid phase.

Plasma generation in water close to the surface can contribute to a greater involvement of particles from the gaseous environment in the interaction of plasma and water, thereby increasing their solubility in water. To realize this process, the plasma generated by the laser in water must also propagate outward. The size of the laser-induced plasma is determined by the Rayleigh length (Z_R), which is defined by

Table 1. Change of pH and Electrical Conductivity Values of Water Depending on the Exposure Time

exposure time (min)	5	10	15	20	25	HNO_3
pH	3.75	3.54	3.26	3.1	2.97	2.96
conductivity, μS/cm	110	161	219	285	344	360

https://doi.org/10.1021/acsomega.2c02384
ACS Omega 2022, 7, 28182−28189

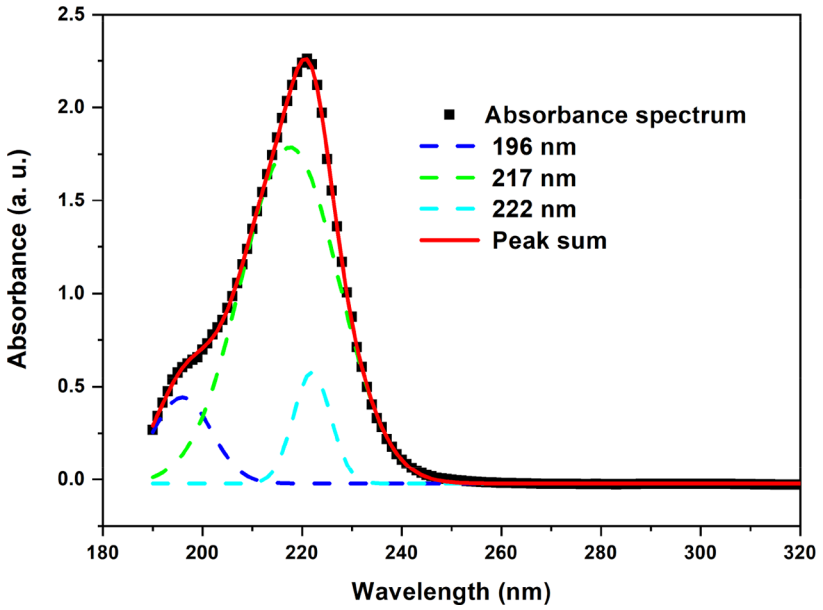

Figure 7. Segregation of the absorbance spectrum of water after 25 min of laser exposure by Gaussian function fitting. It reveals that the peak consists of three peaks.

the waist radius (w_0) and the wavelength (λ) of the laser as given in Figure 6.[30] Inserting the values of a waist radius (w_0) of 50 μm (see the Experimental Section) and a wavelength of the laser of 1030 nm in the equation yields a Rayleigh length of 8 mm and a confocal parameter, which is twice the Raleigh length, of 16 mm. It is also well known that the generated plasma in the liquid can be expanded and increase in its volume by two processes.[23,31] The first process is the thermal expansion around the breakdown site that yields the formation of water bubbles, and the second one is the continued ionization that leads to the formation of a new plasma up the beam path (in the direction of the laser) from the original breakdown site. The generated water vapor, in turn, contributes to the spread of plasma in the air.

The observed dependence of the peak intensity on the focus position of the laser as given in Figure 2 could be explained by the size of the plasma in contact with water. Focusing the laser beam at the water surface led to a slight appearance of nitrogen radicals (low absorbance signal) which indicates small contact between the plasma and water, leading to insufficient ionization of water. A deeper focus of the plasma in water leads to an increase in contact volume of water subjected to the plasma, which results in the formation of more radicals that can react with species dissolving from the gaseous phase in contact with the plasma. Furthermore, the formation of a shock wave by laser plasma in water facilitates the diffusion of the reaction products throughout the entire volume of water. Further increasing the depth of the laser focus in water will result in decreasing its contact with the gaseous phase and hence prevent the formation of gaseous particles that can penetrate into water from air, leading to the observed decrease in peak intensity (Figure 2).

To identify the ions contributing to the observed signal in Figures 2 and 4, the treated water samples were analyzed by IC and are presented in Figure 5. As can be seen from this figure, only one peak appeared in the chromatograph, which corresponds to the NO_3^- anion. The absence of the expected appearance of NO_2^- anions can be explained by their transformation into NO_3^-, which is usually accelerated in acidic conditions.[32] The pH measurements of the treated water showed a decrease in its value with an increase in laser exposure time (Table 1). The observed increase in the concentration of nitrate ions with a simultaneous decrease in pH suggests the formation of nitric acid by laser-induced plasma. This implies that the concentration of nitrate ions and protons in this solution should be equal. To confirm, we have calculated the concentration of protons from the pH value and the concentration of nitrate ions from IC. For 25 min laser-treated water, the pH value was 2.94. This corresponds to a molar concentration of H^+ of 1×10^{-3} mol/L. The measured NO_3^-ion concentration in this solution was 50 mg/L. This corresponds to a nitrate concentration of 0.8×10^{-3} mol/L. These values are in close agreement with each other and hence lend further support to our claim of the formation of nitric acid in the treated water solution.

In order to identify the ions contributing to the observed UV spectra of the laser-treated water, Gaussian function fitting of the absorbance peak was performed, which showed the existence of three signals centered at 196, 217, and 222 nm (Figure 7). These signals can be ascribed to the optical absorption of different forms of NO_3 ions in water.[28] The peak centered at 222 nm could be ascribed to the presence of conjugation of three or more nitrate ions that leads to the formation of trimers, tetramers, or higher order species. The peaks at 217 nm could be ascribed to the existence of monomers and dimers in the solution. These conjugations lead to the observed red shift in the absorption spectra as compared to the spectra of the dilute solution of nitric acid which occurs at λ_{max} of 211 nm (data not shown). The red shift of the absorbance spectrum with increasing laser exposure time can be explained by the formation of a higher order of conjugation, which results in a decrease in the energy gap between the highest occupied molecular orbital and lowest unoccupied molecular orbital in the NO_3 ions.[33] This proposition is supported by the lack of other ions that could be retrieved from IC measurements. Furthermore, hydrogen peroxide (H_2O_2) is excluded from this analysis since its λ_{max} (160 nm) is located outside the wavelength range of the

https://doi.org/10.1021/acsomega.2c02384
ACS Omega 2022, 7, 28182−28189

spectrophotometer.[28] The peak at 196 nm, which appeared even after processing in the Ar gas environment (see Figure 3), did not change its position with increasing laser exposure time and, therefore, was attributed to unknown radicals formed in water during laser irradiation.

4. CONCLUSIONS

The laser-induced plasma−liquid interface provides many fundamental and interesting scientific phenomena such as ionization, sharp explosion, shock wave radiation, bubble creation, and splitting. The coupling of liquid phase plasma kinetics with gas-phase reactivity remains a challenge and requires a systematic study of plasma−liquid−air interactions and subsequent chemical reactions in the liquid phase. In our study, we focused on the effect of the surrounding environment on the processes that occur in water during the generation of laser-induced plasma at the water−gas interface. Plasma was generated in pure water using a femtosecond laser in the presence of different surrounding environments such as air and N_2 and Ar gases. We observed a large number of species from the environment—in particular, nitrate ions—dissolved in water after laser plasma generation near the water surface. Moreover, the number of these species was found to depend on the position of the laser focus in water and on the laser exposure time. The formation of reactive nitrogen (and possible oxygen) species in water can be used for water cleaning and disinfection, which has high impact and tremendous potential in the fields of laser nanosurgery, environmental protection, colloidal chemistry, and gas/liquid solubility. This laser-driven approach can increase the solubility of hydrophobic gases in water at low pressure, which would allow the use of such modified water as a new solvent for green organic chemistry and biology. Moreover, a high solubility of gases in water offers a new and potentially effective way to produce nanobubbles. The high surface area-to-volume ratio of nanobubbles can enhance the rates of gas solution reactions[34] and may play an important role in a host of biological phenomena and processes.[35]

AUTHOR INFORMATION

Corresponding Author

Ali S. Alnaser − *Department of Physics, American University of Sharjah, Sharjah 26666, UAE;* orcid.org/0000-0003-4822-9747; Email: aalnaser@aus.edu

Authors

Vadim Ialyshev − *Department of Physics, American University of Sharjah, Sharjah 26666, UAE*

Ganjaboy Boltaev − *Department of Physics, American University of Sharjah, Sharjah 26666, UAE*

Mazhar Iqbal − *Department of Physics, American University of Sharjah, Sharjah 26666, UAE*

Mustafa Khamis − *Department of Biology, Chemistry and Environmental Sciences, American University of Sharjah, Sharjah 26666, UAE*

Complete contact information is available at: https://pubs.acs.org/10.1021/acsomega.2c02384

Notes

The authors declare no competing financial interest.

This paper represents the opinions of the authors and does not mean to represent the position or opinions ofthe American University of Sharjah.

ACKNOWLEDGMENTS

This study was supported by the FRG grant # FRG19-L-S61 from the American University of Sharjah, United Arab Emirates. The work in this paper was supported, in part, by the Open Access Program from the American University of Sharjah.

REFERENCES

(1) Stan, C.-A.; Milathianaki, D.; Laksmono, H.; Sierra, R.-G.; McQueen, T.-A.; Messerschmidt, M.; Williams, G.-J.; Koglin, J.-E.; Lane, T.-J.; Hayes, M.-J.; Guillet, S.-A.-H.; Liang, M.; Aquila, A.-L.; Willmott, P.-R.; Robinson, J.-S.; Gumerlock, K.-L.; Botha, S.; Nass, K.; Schlichting, I.; Shoeman, R.-L.; Stone, H.-A.; Boutet, S. Liquid explosions induced by x-raylaser pulses. *Nat. Phys.* **2016**, *12*, 966.

(2) Silberberg, Y. Laser science: Physics at the attosecond frontier. *Nature* **2001**, *414*, 494.

(3) Gattass, R.-R.; Mazur, E. Femtosecond laser micromachining in transparent materials. *Nat. Photonics* **2008**, *2*, 219.

(4) Linz, N.; Freidank, S.; Liang, X.-X.; Vogelmann, H.; Trickl, T.; Vogel, A. Wavelength dependence of nanosecond infrared laser-induced breakdown in water: Evidence for multiphotoninitiation via an intermediate state. *Phys. Rev. B: Condens. Matter Mater. Phys.* **2015**, *91*, 134114.

(5) Vogel, A.; Venugopalan, V. Mechanisms of pulsed laser ablation of biological tissues. *Chem. Rev.* **2003**, *103*, 577−644.

(6) Williamson, J.-C.; Cao, J.; Ihee, H.; Frey, H.; Zewail, A.-H. Clocking transient chemicalchanges by ultrafast electron diffraction. *Nature* **1997**, *386*, 159.

(7) Sundaram, S.-K.; Mazur, E. Inducing and probing non-thermal transitions in semiconductors using femtosecondlaser pulses. *Nat. Mater.* **2002**, *1*, 217−224.

(8) Sokolowski-Tinten, K.; Bialkowski, j.; Cavalleri, A.; von der Linde, D.; Oparin, A.; Meyer-ter-Vehn, J.; Anisimov, S.-I. Transient states of matter during short pulse laser ablation. *Phys. Rev. Lett.* **1998**, *81*, 224−227.

(9) Alghabra, M.-S.; Ali, R.; Kim, V.; Iqbal, M.; Rosenberger, P.; Mitra, S.; Dagar, R.; Rupp, P.; Bergues, B.; Mathur, D.; Kling, M.-F.; Alnaser, A.-S. Anomalous formation of trihydrogen cations from water on nanoparticles. *Nat. Commun.* **2021**, *12*, 3839.

(10) Pichat, P. A brief overview of photocatalytic mechanisms and pathways in water. *Water Sci.Technol.* **2007**, *55*, 167.

(11) Ikeda, T.; Fujiyoshi, S.; Kato, H.; Kudo, A.; Onishi, H. Time-Resolved Infrared Spectroscopy of K3Ta3B2O12 Photocatalysts for Water Splitting. *J. Phys. Chem. B* **2006**, *110*, 7883.

(12) Bonev, B. P.; Mumma, M. J.; DiSanti, M. A.; Dello Russo, N.; Magee-Sauer, K.; Ellis, R. S.; Stark, D. P. A Comprehensive Study of Infrared OH Prompt Emission in Two Comets. I. Observations and Effective g-Factor. *Astrophys. J.* **2006**, *653*, 754.

(13) Maeda, K.; Domen, K. New Non-Oxide Photocatalysts Designed for Overall Water Splitting under Visible Light. *J. Phys. Chem. C* **2007**, *111*, 7851.

(14) Kierzkowska-Pawlak, H.; Tyczkowski, J.; Jarota, A.; Abramczyk, H. Hydrogen production in liquid water by femtosecond laser-induced plasma. *Appl. Energ* **2019**, *247*, 24−31.

(15) Soong, H.-K.; Malta, J.-B. Femtosecond lasers in ophthalmology. *Am. J. Ophthalmol.* **2009**, *147*, 189−197.

(16) Grewal, D.-S.; Schultz, T.; Basti, S.; Dick, H.-B. Femtosecond laser−assisted cataract surgery−current status and future directions. *Surv. Ophthalmol.* **2016**, *61*, 103−131.

(17) Rehse, S.-J.; Salimnia, H.; Miziolek, A.-W. Laser-induced breakdown spectroscopy (LIBS): an overview of recent progress and future potential for biomedical applications. *J. Med. Eng. Technol.* **2012**, *36*, 77−89.

(18) Lazic, V.; Jovicevic, S.; Fantoni, R.; Colao, F. Efficient plasma and bubble generation underwater by an optimized laser excitation and its application for liquid analyses by laser-induced breakdown spectroscopy. *Spectrochim. Acta, Part B* **2007**, *62*, 1433.

(19) Bruggeman, P.; Kushner, M.-J.; Locke, B.-R.; Gardeniers, J.-G.; Graham, W.; Graves, D.-B.; et al. Plasma−liquid interactions: a review and roadmap. *Plasma Sources Sci. Technol.* **2016**, *25*, 053002.
(20) Cao, Y.; Qu, G.; Li, T.; Jiang, J.; Wang, T. Review on reactivespecies in water treatment using electrical discharge plasma: formation, measurement, mechanisms and mass transfer. *Plasma Sci. Technol.* **2018**, *20*, 103001.
(21) Xu, J.; Chen, D.; Meng, S. Probing Laser-Induced Plasma Generation in Liquid Water. *J. Am. Chem. Soc.* **2021**, *143*, 10382−10388.
(22) Chin, S.-L.; Lagace, S. Generation of H_2, O_2, and H_2O_2 from water by the use of intense femtosecond laser pulses and the possibility of laser sterilization. *Appl. Opt.* **1996**, *35*, 907−911.
(23) Kennedy, P.-K.; Hammer, D.-X.; Rockwell, B.-A. Laser-inducedbreakdown in aqueous media. *Prog. Quantum Electron.* **1997**, *21*, 155−248.
(24) Garrett, B.-C.; Dixon, D.-A.; Camaioni, D.-M.; Chipman, D.-M.; Johnson, M.-A.; Jonah, C.-D.; et al. Role of water in electron-initiated processes and radical chemistry: Issues and scientific advances. *Chem. Rev.* **2005**, *105*, 355−390.
(25) Khan, S.-A.; Boltaev, G.-S.; Iqbal, M.; Kim, V.; Ganeev, R.-A.; Alnaser, A.-S. Ultrafast fiber laser-induced fabrication of super-hydrophobic and self-cleaning metal surfaces. *Appl. Surf. Sci.* **2021**, *542*, 148560.
(26) Le Caër, S.; Rotureau, P.; Brunet, F.; Charpentier, T.; Blain, G.; Renault, J.-P.; Mialocq, J.-C. Radiolysisof confined water: Hydrogen production at a high dose rate. *ChemPhysChem* **2005**, *6*, 2585.
(27) Kumar, A.; Kołaski, M.; Lee, H.-M.; Kim, K.-S. Photoexcitation and Photoionization Dynamics of Water Photolysis. *J. Phys. Chem. A* **2008**, *112*, 5502−5508.
(28) Oh, J.-S.; Szili, E.-J.; Ogawa, K.; Short, R.-D.; Ito, M.; Furuta, H.; Hatta, A. UV−vis spectroscopy study of plasma-activated water: Dependence of the chemical composition on plasma exposure time and treatment distance. *Jpn. J. Appl. Phys.* **2018**, *57*, 0102B9.
(29) Bruggeman, P.; Leys, C. Non-thermal plasmas in and in contact with liquids. *J. Phys. D: Appl. Phys.* **2009**, *42*, 053001.
(30) Damask, J.-N. *Polarization Optics in Telecommunications*; Springer: New York, 2004; pp 221.
(31) Song, J.; Guo, J.; Tian, Y.; Xue, B.; Lu, Y.; Zheng, R. Investigation of laser-induced plasma characteristics in bulk water under different focusing arrangements. *Appl. Opt.* **2018**, *57*, 1640.
(32) Lukes, P.; Dolezalova, E.; Sisrova, I.; Clupek, M. Aqueous-phase chemistry and bactericidal effects from an air discharge plasma in contact with water: evidence for the formation of peroxynitrite through a pseudo-second-order post-discharge reaction of H_2O_2 and HNO_2. *Plasma Sources Sci. Technol.* **2014**, *23*, 015019.
(33) Yanagisawa, S.; Yasuda, T.; Inagaki, K.; Morikawa, Y.; Manseki, K.; Yanagida, S. Intermolecular Interaction as the Origin of Red Shifts in Absorption Spectra of Zinc-Phthalocyanine from First-Principles. *J. Phys. Chem. A* **2013**, *117*, 11246−11253.
(34) Alheshibri, M.; Qian, J.; Jehannin, M.; Craig, V.-S.-J. A history of nanobubbles. *Langmuir* **2016**, *32*, 11086−11100.
(35) Vasa, P.; Mathur, D. *Ultrafast Biophotonics*; Springer: Berlin, 2016.

https://doi.org/10.1021/acsomega.2c02384
ACS Omega 2022, 7, 28182−28189